







Role of geochemical protoenzymes (geozymes) in primordial metabolism: specific abiotic hydride transfer by metals to the biological redox cofactor NAD⁺

Delfina P. Henriques Pereira¹ , Jana Leethaus¹, Tugce Beyazay² ,
 Andrey do Nascimento Vieira¹ , Karl Kleinermanns³, Harun Tüysüz² , William F. Martin¹ 
 and Martina Preiner^{4,5} 

¹ Institute for Molecular Evolution, Heinrich Heine University, Düsseldorf, Germany

² Max-Planck-Institut für Kohlenforschung, Mülheim an der Ruhr, Germany

³ Institute for Physical Chemistry, Heinrich Heine University, Düsseldorf, Germany

⁴ Department of Ocean Systems, Royal Netherlands Institute for Sea Research, Den Burg, The Netherlands

⁵ Department of Earth Sciences, Utrecht University, The Netherlands

Keywords

cofactors; electron donors; hydrogen;
 hydrogenase; NADH; origin of life;
 reduction; serpentinizing systems

Correspondence

M. Preiner, Department of Ocean Systems,
 Royal Netherlands Institute for Sea
 Research, 1790 AB Den Burg and
 Department of Earth Sciences, Utrecht
 University, 3584 CD Utrecht,
 The Netherlands
 Tel: +31 30 253 1409
 E-mail: martina.preiner@nioz.nl

(Received 18 November 2021, revised 9
 December 2021, accepted 17 December
 2021)

doi:10.1111/febs.16329

Hydrogen gas, H₂, is generated in serpentinizing hydrothermal systems, where it has supplied electrons and energy for microbial communities since there was liquid water on Earth. In modern metabolism, H₂ is converted by hydrogenases into organically bound hydrides (H[−]), for example, the cofactor NADH. It transfers hydrides among molecules, serving as an activated and biologically harnessed form of H₂. In serpentinizing systems, minerals can also bind hydrides and could, in principle, have acted as inorganic hydride donors—possibly as a geochemical protoenzyme, a ‘geozyme’—at the origin of metabolism. To test this idea, we investigated the ability of H₂ to reduce NAD⁺ in the presence of iron (Fe), cobalt (Co) and nickel (Ni), metals that occur in serpentinizing systems. In the presence of H₂, all three metals specifically reduce NAD⁺ to the biologically relevant form, 1,4-NADH, with up to 100% conversion rates within a few hours under alkaline aqueous conditions at 40 °C. Using Henry’s law, the partial pressure of H₂ in our reactions corresponds to 3.6 mM, a concentration observed in many modern serpentinizing systems. While the reduction of NAD⁺ by Ni is strictly H₂-dependent, experiments in heavy water (²H₂O) indicate that native Fe can reduce NAD⁺ both with and without H₂. The results establish a mechanistic connection between abiotic and biotic hydride donors, indicating that geochemically catalysed, H₂-dependent NAD⁺ reduction could have preceded the hydrogenase-dependent reaction in evolution.

Introduction

Hydrogen (H₂) is the main source of electrons for chemoautotrophic, industrial, and geochemical CO₂ fixation [1–3]. There are two main sources of naturally

occurring H₂: abiotic geochemical production (serpentinization) and biotic biochemical production via hydrogenases in fermentations. Today, anaerobic autotrophs

Abbreviations

¹H-NMR, proton nuclear magnetic resonance, an analytical method to characterise and quantify hydrogen-containing molecules; Co, cobalt; Fd_{ox}/Fd_{red}, oxidised/reduced ferredoxins; Fe, iron; LUCA, the last universal common ancestor, a theoretical cell based on phylogenetic reconstructions of the most conserved genetic setup between bacteria and archaea; NAD⁺/NADH, oxidised and reduced form of nicotinamide adenine dinucleotide; Ni, nickel.

such as methanogens grow mainly from H₂ of biotic origin, approximately 150 million tons of H₂ per year are produced by microorganisms and consumed by methanogens [4,5]. Only a small fraction of primary production is attributable to chemolithoautotrophy from H₂ geochemically generated during serpentinization in hydrothermal systems [5]. When the first microbial lineages evolved, however, abiotic H₂ was probably the major source of electrons for primary production in ancient ecosystems and metabolism [5–8].

Making the electrons of H₂ accessible

In the absence of effective catalysts, hydrogen is a surprisingly unreactive gas. It can only become chemically or biochemically useful when it is activated, that is, when its covalent bond is broken and the two H-atoms are separated [9]. The homolytic cleavage of gas-phase H₂ that breaks the H–H bond into two H atoms (H·) is endergonic by +436 kJ·mol^{−1} [5,10]. The heterolytic cleavage into a hydride ion (H[−]) and a proton (H⁺) is less endergonic [5,10] but still requires +200 kJ mol^{−1}.

Metal and mineral surfaces can adsorb H₂ both as a molecule by physisorption and as H-atoms by dissociative chemisorption [11–14]. Physisorption of H₂ usually requires very little energy (3–5 kJ·mol^{−1}) so it is most easily observed at low temperature in the range of liquid helium [14]. For chemisorption, hydrogen has to overcome the activation barrier and thus higher temperatures are usually required to form the metal-bound hydride, depending on the material. If the kinetic energy of the H₂ molecule is high enough, it can be dissociated directly on the surface of a suitable catalyst. But indirect chemisorption starting from the transient physisorbed state is also possible; physisorbed H₂ molecules can diffuse quickly on catalyst surfaces and then dissociate when the right catalytic site is met [3,14–16].

Microbes solved the problem of H₂ activation and cleavage about 4 billion years ago with the origin of hydrogenases, enzymes that dissociate H₂ into two protons and two electrons. H₂ was the source of electrons for primary production before photosynthesis emerged [8] and hydrogenases were already present in the last universal common ancestor (LUCA) [17]. All hydrogenases known catalyse a reversible reaction such that they can either use H₂ as an electron source or dispose of leftover electrons as H₂. There are three different kinds of hydrogenases, all of them holding transition metals coordinated by varying ligands in their active sites: [NiFe], [FeFe] and [Fe] [4,18–20]. Most of the reaction intermediates in the active site of hydrogenases have been determined [20]. All three perform a heterolytic cleavage of H₂, but do so in mechanistically

different ways; the same applies to the reverse reaction, the formation of H₂. The bond is polarised at an open metal site, such that a proton (H⁺) is accepted by a nearby base ligand, while the hydride (H[−]) remains bound to the metal, transiently altering its oxidation state. In the case of [FeFe] hydrogenases, H[−] is bound end-on to one of the two Fe atoms [9,20,21]. In [NiFe] hydrogenases, H[−] binds to both Ni and Fe (with help of an extra electron coming from Ni), making the hydride more stable than the one in [FeFe] hydrogenases [9,20,21]. The mechanism of [Fe] hydrogenases involves a direct hydride transfer from H₂ to an organic substrate, in contrast to the other two hydrogenases which need the assistance of FeS centres for this procedure [22].

Hydride carriers in biology

Though the reaction mechanisms of hydrogenases differ, their result is similar: Electrons from H₂ are transferred to soluble electron acceptors such as NAD⁺, F₄₂₀, or iron-sulfur clusters of oxidised ferredoxins (Fd_{ox}) for entry into metabolism [23]. While NAD and F₄₂₀ donate and accept electron pairs as hydrides (two-electron reactions), ferredoxin donates and accepts single electrons (one-electron reactions). In this paper, we focus on NAD and the H[−]-transfer reaction that reduces its oxidised form, NAD⁺, to its reduced form NADH [24,25]. NADH is a universal redox cofactor present in all cells, it is one of the most central molecules of metabolism, being essential in autocatalytic metabolic networks, meaning that without NADH metabolism cannot take place [26].

While hydrogenases make the electrons of H₂ accessible in modern cells [1,5,27], at the emergence of metabolism, before the existence of enzymes, electrons from H₂ that participated in CO₂ reduction and organic synthesis must have been activated by inorganic means such as mineral and metal surfaces [28–31]. Minerals could have served as prebiotic protohydrogenases ('geozymes') producing surface-bound hydrides (e.g. Fe–H) from dissociated H₂ which, in turn, are a prebiotic version of NADH. That this abiotic catalysis works for the reduction of CO₂ was shown previously [32,33]. Here our question was whether geochemical hydrides can reduce NAD⁺ to NADH which could have served as a soluble electron carrier at the origin of metabolic pathways. The existence of soluble electron carriers at origins is of interest for early metabolic evolution because catalytically active sites on minerals are immobile, whereas soluble organic hydride carriers such as NADH can transport activated H to mineral surfaces that might, for

example, catalyse organic redox reactions but not H₂ activation *in situ*.

Connecting geochemical with biological hydride carriers

To address possible transition points between abiotic and biotic hydride donation and the question of why NAD⁺/NADH became one of the universal hydride donors and acceptors in metabolism, we investigated geochemical conditions under which NAD⁺/NADH can (a) accept (and donate) hydrides and (b) remain stable. From earlier studies, it is known that NAD⁺ can be reduced heterogeneously on industrial catalysts [34,35] at neutral to slightly alkaline pH, so an approach under more rugged and natural conditions seemed possible. In a prebiotic context, this would entail a constant supply of environmental H₂ and accessible mineral surfaces. Serpentinizing systems harbour geochemical sites that reduce H₂O to H₂ via the oxidation of Fe(II)-containing minerals and thus provide these conditions [36,37]. Most but not all of these systems are alkaline because of the accumulation of metal hydroxides during serpentinization reactions [36,38]. Some microbes inhabiting such environments appear to lack hydrogenase enzymes [39], suggesting that even today, there might be alternative (abiotic?) and probably metal-based entry points for H₂ into metabolism.

To reduce NAD⁺ with H₂, we investigated three different metals as potential H₂ activating agents: Fe, Co and Ni. We started with native metals to keep the reactions as simple as possible. Both Fe and Ni are employed in the active centres of hydrogenases, but are also found in serpentinizing systems in oxidised and reduced forms [40,41]. We included Co because it is a crucial transition metal in autotrophic CO₂ fixation [1] and it is assumed to have been abundant in the Archean anoxic ocean [42]. In addition, Co complexes are being tested for its properties as artificial hydrogenases [43]. The hydrides of all three metals are known to have approximately the same hydricity (tendency to transfer hydrides) [44] as NADH and are ultimately direct neighbours in the periodic system of elements, so this choice of metals would also allow us to set their experimental behaviour in relation to their electrochemical potential.

Results

NAD⁺ reduction with H₂ and transition metals under alkaline conditions

We used conditions approximating those found in alkaline serpentinizing systems (starting pH 8.5, 5 bar

H₂ atmosphere, 40 °C), with metals Fe, Ni and Co [40,45] in powdered form, (1 M). The resulting aqueous H₂ concentration of 3.6 mM (calculated using Henry's law, s. Equation S1) is comparable to that found in hydrothermal effluent [38,40]. Under these conditions, the reduction of 3 mM NAD⁺ to NADH was facile (Fig. 1A,B). Fe, Ni and Co also play important catalytic roles in autotrophic metabolism [46–48]. That all three metals promote the reaction between NAD⁺ and H₂ to NADH was observed with ¹H-NMR, enabling us to make a detailed structural determination of our products as various prospective hydride acceptor sites exist on the NAD⁺ molecule and also degradation products such as nicotine amide are possible [49,50]. Our results show that indeed the biological form of NADH, 1,4-NADH, was the main product. We also observe some degradation products (mainly nicotinamide), but in low concentrations under the reaction conditions tested.

In order to probe the nature of H₂–metal interactions in these reactions, we performed four different experiments with each metal (for visual overview s. Fig. S1). In two reactions, we first pretreated the metal powders in a dry state with H₂ gas for 16 h at 50 °C before adding a buffer/NAD⁺ solution. Chemisorption and dissociation of H₂ is feasible at these temperatures [51–53]. This approximates the situation in serpentinizing systems, where H₂ is being produced continuously, such that the minerals could be constantly hydrogenated (i.e. organic redox cofactors and not hydrogenated minerals would be rate-limiting in the geochemical reaction). In addition, and in accordance with previous industrial investigations of heterogeneous NAD⁺ reduction [35], a thermal (> 350 °C) pretreatment of the catalyst with H₂ increased the yield of reduced NADH due to more or less saturating hydrogenation of the catalyst. Pretreated and non-pretreated metal powders were mixed with the phosphate buffer/NAD⁺ solution and reactions from 0.5 to 4 h were performed either under 5 bar of Ar or H₂ at 40 °C. In the Ar experiments, NAD⁺ reduction can be attributed to the activity of preformed hydrides on the metal surface. Controls without metals were conducted in each run, showing that metals are needed for the reduction of NAD⁺. All experiments were repeated at least three times. All the corresponding spectra can be found in Fig. S2.

The results summarised in Fig. 2 show how each metal responds to the different experiments over a 4-h course. The corresponding table with all individual measurements and standard deviation values can be found in the supplementary information (Table S1). Pretreating the metals with H₂ has a positive effect on

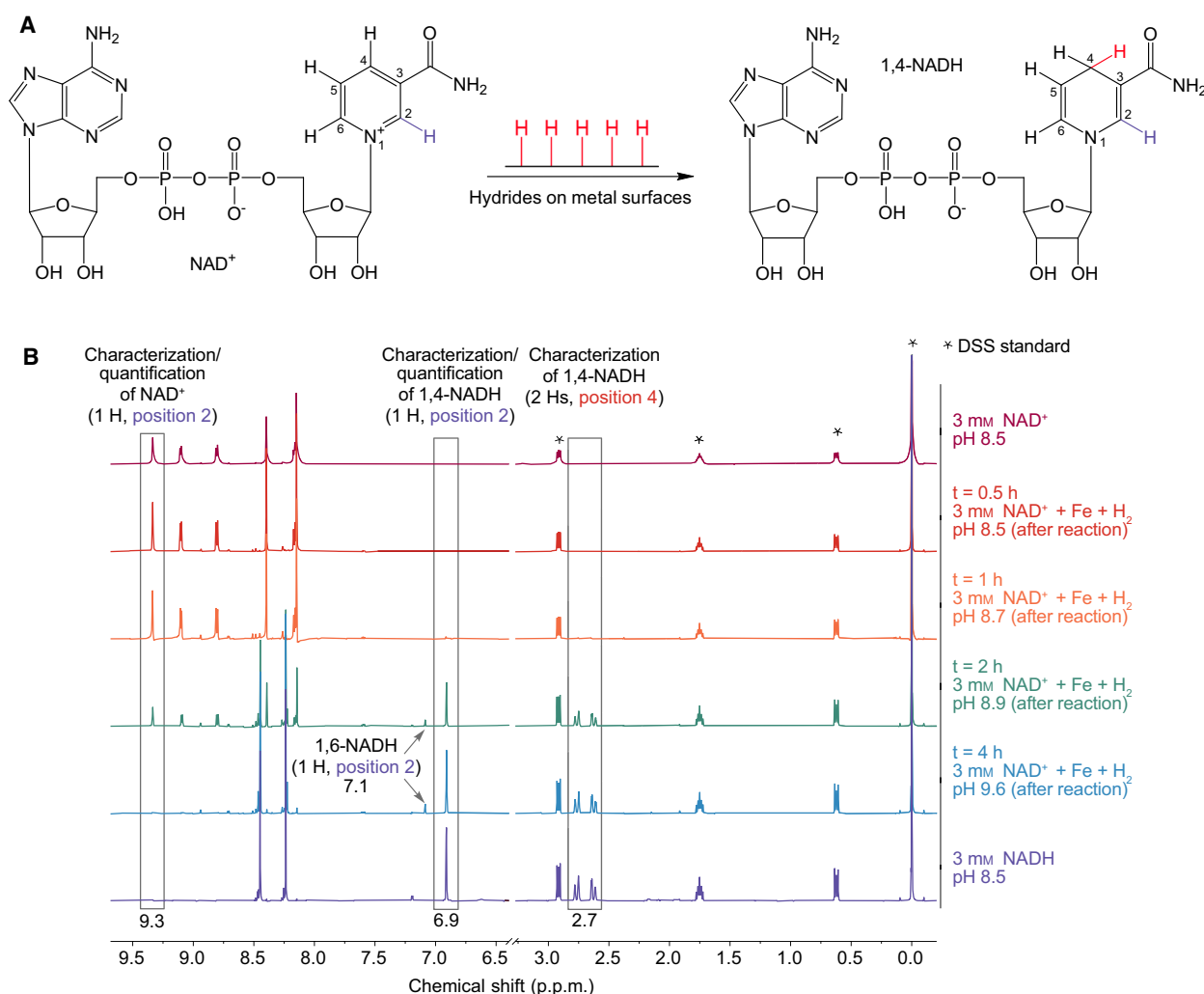


Fig. 1. Reduction of NAD⁺ with H₂ and Fe powder over time. (A) NAD⁺ is reduced to 1,4-NADH, the naturally occurring reduced form of nicotinamide adenine dinucleotide (NAD). This means a hydride is added to the carbon in position 4 of the aromatic cycle of NAD⁺. NAD⁺ can also be reduced at two further positions, the second and the sixth, thus leading to 1,2-NADH and 1,6-NADH respectively [84]. (B) Within 4 h, NAD⁺ is reduced to 1,4-NADH as monitored via ¹H-NMR. A pH shift from 8.5 to 9.6 is observed, probably due to the oxidation of Fe powder coupled to the reduction of H₂O to hydrides/H₂ (accumulation of OH⁻). The peaks of the used NMR standard sodium trimethylsilylpropanesulfonate (DSS) are marked with asterisks.

the NAD reducing activity of all three metals: Fe reaches high NADH yields quickly (Fig. 2A), as does Co (Fig. 2B), but the clearest effect can be seen with Ni, where only with H₂-pretreatment NADH yields approaching 50% can be reached. With both Fe and Co nearly 100% conversion from NAD⁺ to NADH is observed, but with one important difference: while Co clearly needs H₂ gas during the reaction to reach a high yield of NADH, Fe shows almost identical results under Ar as it does under H₂. Under Ar, Co can still convert almost 50% of NAD⁺ to NADH. The amount of metal used in comparison to NAD⁺ is very high (1 M of metal to 3 mM NAD⁺, so 333 : 1), but

experiments with a ratio of 20 : 1 (62.5 mM to 3 mM NAD⁺) and 10 : 1 (62.5 mM to 6 mM NAD⁺) (Fig. S3) showed that all three metals still yield NADH at the lower ratios. While Fe yields about 40% NADH at 10 : 1, Ni only reaches 0.6% at the same metal to NAD⁺ ratio.

We also observed a significant pH increase (s. Fig. S4) during the Fe and Co reactions and the development of coloured colloids (Fe: dark green, Co: pink; s. Fig. S5), especially when there was no H₂ gas added to the reaction or when not pretreated with H₂, while the pH remained stable and the solution colloid free (though coloured yellow) during the Ni reactions. The

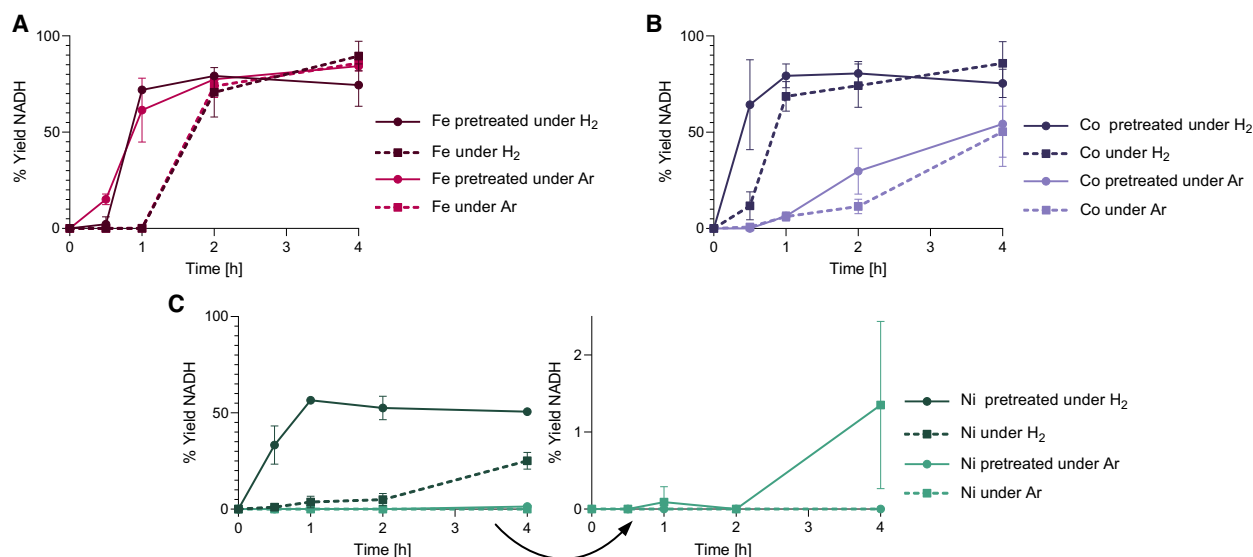


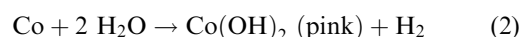
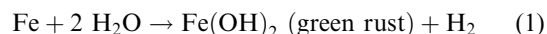
Fig. 2. NADH synthesis with Fe, Co and Ni under four different settings. In the experiments, the three metal powders were either pretreated with H₂ gas overnight at 50 °C before the reactions under 5 bar H₂ or Ar between 0.5 and 4 h (solid lines and circles), or the reactions took place without the pretreatment (dashed lines and squares). Data points shown are mean \pm SD. (A) Fe does not need an external H₂ source under the given conditions, NADH synthesis is equally efficient in both cases. Pretreated Fe reduces NAD⁺ faster but does not lead to a higher yield overall. Repetitions from 0.5 h to 4 h: n(pretreated, H₂) = 3, 3, 4, 3; n(H₂) = 3, 4, 4, 6; n(pretreated, Ar) = 2, 3, 2, 3; n(Ar) = 1, 4, 3, 3. (B) Co can reduce up to roughly 50% of NAD⁺ without an external H₂ source, but the presence of H₂ gas improved the yield and accelerated the conversion immensely. Pretreatment with H₂ also decreased the reaction time of the conversion visibly as long as there is an H₂ source during the reaction. Repetitions from 0.5 h to 4 h: n(pretreated, H₂) = 4, 4, 4, 4; n(H₂) = 4, 4, 4, 5; n(pretreated, Ar) = 2, 5, 4, 6; n(Ar) = 4, 4, 4, 4. (C) Ni powder cannot reduce NAD⁺ under the absence of H₂ as an electron source. Pretreated with H₂, Ni shows a 50% yield of NADH. Pretreated Ni can convert a very small amount of NAD⁺ to NADH under Ar, suggesting that hydrides are covering the surface of the metals after the pretreatment. Repetitions from 0.5 h to 4 h: n(pretreated, H₂) = 4, 3, 3, 4; n(H₂) = 4, 4, 4, 6; n(pretreated, Ar) = 2, 5, 4, 6; n(Ar) = 0, 4, 4, 4.

pH shift observed was also the reason we chose to work with a 1 M phosphate buffer. With buffers of lower concentrations, the pH of the Fe and Co samples shifted far into the alkaline range (> pH 10 and > pH 9 respectively), conditions under which NAD⁺ is unstable and decomposes [54] (s. Figs. S6, S7A). NADH, however, is far more stable under alkaline conditions, as we were able to determine in additional experiments, the results of which are summarised in Fig. S7B. The phosphate buffer can, however, lead to a degradation of NADH [55], which can explain minor losses we observed in NAD⁺ conversion (Table S1).

These observations led us to the conclusion that while Ni clearly catalysed the dissociation of H₂ gas and is thus making electrons from H₂ accessible to NAD⁺, both Fe and Co themselves can serve as the electron source instead of H₂ gas and are being oxidised (directly connected to the developing colouration), especially during the experiments without external H₂ source (under Ar). We undertook additional experiments to further investigate the role of Fe and Co as reductants.

Probing the role of metals with ²H: H₂ activation, H₂ synthesis, both or something else?

The observed pH shifts and colouration were a hint for following redox reactions taking place (the hydroxides generated are partly soluble [56] and lead to an pH increase):



Fe and Co powder are able to produce nascent H₂: freshly synthesised H₂ from two hydrogen atoms. The intermediates of this reaction are surface-bound hydrides [57] which could, in theory, be directly transferred to NAD⁺. It is also known that Fe readily produces H₂ from water under mild alkaline conditions [58]. To clarify the present mechanisms, Fourier-transform infrared spectroscopy (FTIR) was performed on all three metals (Fe, Co and Ni) before and after the reaction under Ar (expecting the highest

oxidation rate in these experiments in contrast to the ones under H₂ gas and hence more reducing conditions). The respective FTIR spectra (s. Fig. S8) show the differences between the metals very clearly, in line with our other results. Ni does not show any visible changes, Co does, but not clearly enough to specify the nature of the change. The spectrum of Fe after the reaction shows a new Fe-O bond (in the region of 500–600 cm⁻¹) as well as stretching and bending bands of -OH groups located around 3200 and 950 cm⁻¹ respectively, which indicates transformation of metallic iron into iron hydroxides such as Fe(OH)₂, confirmed by the dark green colouration of the Fe samples ('green rust').

To further probe the mechanisms of NAD⁺ reduction, we replaced H₂O in the solvent with heavy water (²H₂O, D₂O) to determine the source of the hydrides added to NAD⁺. There were two reasonable options: either protons from H₂O and metal electrons (formed

to surface-bound hydrides) or surface-bound hydrides from H₂ gas. Previous work on reducing NAD⁺ and ²H sources [59,60] provided us with mechanistic details and reference ¹H-NMR spectra for NAD²H species, the presence of which can be monitored via the duplet of duplet at 2.7 p.p.m. (position 4 as shown in Fig. 1). In our case, we would expect the formation of NAD²H instead of NADH if the hydride comes from ²H⁺ in ²H₂O plus electrons from metal, while NADH should be formed if the H₂ gas is the prevalent hydride source. Three 2-hour NAD⁺ reduction experiments with Fe, Co and Ni were performed in ²H₂O (otherwise using the same conditions as described above): metals under Argon, H₂-pretreated metals under Argon and metals under H₂. The results are shown in Fig. 3 with a focus on the 2.7 p.p.m. peaks described above (s. Fig. S2 to see the full range of the shown spectra). When no (under Argon Fig. 3A) or only little H₂ (pretreated and reaction under Argon, Fig. S9 and

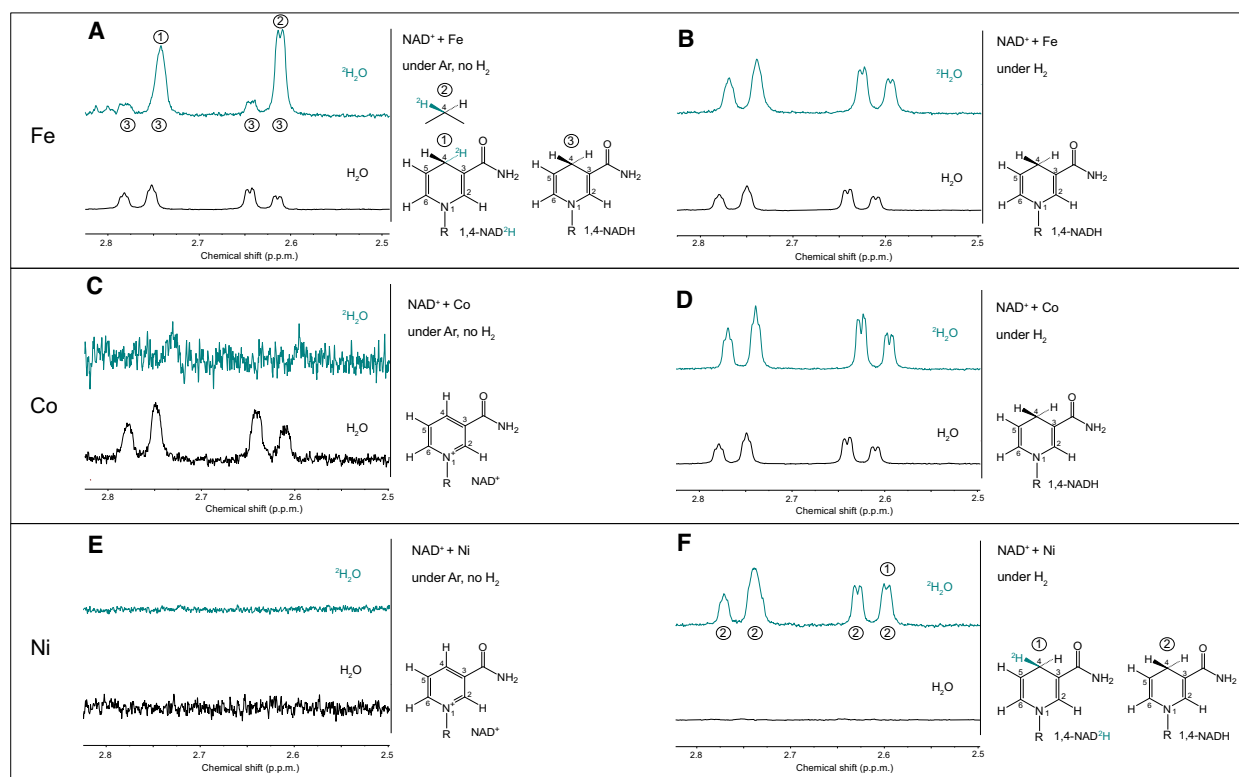


Fig. 3. Two-hour experiments in ²H₂O to determine the source of the H⁻ reducing NAD⁺. (A) When there is no external H₂ source, Fe delivers the electrons to form ²H⁻ from ²H₂O which is transferred to NAD⁺. The Deuterium (²H) at position 4 in the nicotinamide ring of NADH changes the proton coupling visibly. (B) The mechanism for NADH formation apparently changes when H₂ is added to the reaction. NADH becomes the main product, suggesting that H₂ is catalytically activated by Fe. (C) Co does not produce NAD²H (or NADH) over the detection limit under Ar gas in ²H₂O. (D) When H₂ is added to the reaction, Co promotes NADH formation. (E) Ni does not produce NAD²H (or NADH) over the detection limit under Ar gas in ²H₂O (or ¹H₂O). (F) In contrast to the ¹H₂O experiments, Ni highly promotes NADH formation in ²H₂O under H₂ after 2 h. Note that (C) and (E) are more vertically zoomed in than the rest of the panels as the product concentration was significantly lower.

Table S1) is in the experimental system, NAD²H is the prevalent product of the reactions with Fe. This indicates that Fe reduces ²H₂O to ²H[−] which then is transferred to NAD⁺. When the reaction is performed under ¹H₂ atmosphere (Fig. 3B), however, the product does not contain any measurable amount of ²H, suggesting that ¹H₂ is the hydride source in this case. We confirmed these observations additionally by integrating the duplet of duplet at 2.7 p.p.m. in both the Ar and the H₂ experiments (the peak integrals correspond to the number of associated ¹H; ²H is not detected). The integral values were compared to those of the singlet at 6.9 (1 ¹H-proton), ultimately showing that in ²H₂O and under Ar only one ¹H-proton is detected at position 4 of NADH (Table S2). In combination with the other findings above, the reaction path involving Fe-dependent reduction of water (or ²H₂O) to metal-bound hydride (or ²H[−]) appears reasonable. Fe seems to employ both described mechanisms, depending on the conditions. The positive effect of Fe pretreatment with H₂ is not explained by the present results. However, it is worth to mention that the overall yield of NADH with Fe under Ar is substantially lower and variable in ²H₂O (0–50%, Table S1) than it is in ¹H₂O (60–70%), while pretreatment increases the yield of NAD²H in the ²H₂O experiments (~80%, Table S1). We still registered a pH shift and slight green colouration suggesting the formation of Fe(OH)₂ (Figs. S4, S5). We will return to this observation shortly.

Cobalt does not deliver a picture as clear as that obtained for Fe. H₂ was necessary during the Co catalysed reaction to detect NADH formation in the ²H₂O experiments. Co reduces NAD⁺ to NADH under Ar, without H₂ and with ¹H₂O as proton source (Fig. 3C, lower trace), although with a far lower yield than Fe (Fig. 2B or Table S1). In the ²H₂O experiments however, H₂ was necessary for NADH formation. We could not observe any NAD²H formation after 2 h (Fig. 3D). Performing the same experiment for 4 h yielded detectable amounts of NADH, but not enough to investigate the peak at 2.7 p.p.m. (Table S1) and thus the status of deuteration.

In the case of Ni, the experiments under Ar confirm the conclusion from the previous experiments (no NADH formation). Nevertheless, a surprising effect of ²H₂O was observed: while only very little NADH formation was observed after 2 h in H₂O under H₂, almost all NAD⁺ is converted to NADH in ²H₂O (Fig. 3F) and there seems to be a very small amount of NAD²H formed. We have no thorough explanation for this puzzling observation, but it is possible that H₂O absorbing on the Ni surface occupies sites needed for H₂ dissociation—while ²H₂O does not as easily

[61–63]. The formation of NAD²H is probably the result of an exchange between H⁺ and ²H⁺ as the peak distribution is by far not as clear as in the case of Fe (Fig. 3A).

Overall, we were able to derive some valuable conclusions from the experiments performed under ²H₂O, but there are also some observations (e.g. yield loss with Fe and Co) that we cannot properly explain so far and are most likely the result of isotopic effects.

Being aware that metal ions are going into solution during our experiments, we also tried to exclude these dissolved species as being the true catalysts in our reactions. Therefore, we performed a ‘hot filtration test’ for all metals, that is, we separated the solid from the liquid phase after a 1 h reaction under H₂ (so we could test whether hydride-bearing, soluble complexes are being formed), added a new NAD⁺/buffer solution onto the solid phase and resumed the reaction under 5 bar for both parts for another 1 h and compared the NADH yields (Fig. S10). The separated liquid phase did not show any additional NADH formation for any of the metals, while the separated solid phase was still able to promote a very high NAD⁺ → NADH transformation yield (95% for Fe, 81% for Co, 35% for Ni after 1 h of reaction time). This indicates that the solid metals are the (far) more crucial species for NAD⁺ reduction in our experiments.

In addition, we also observed that the reaction with fresh NAD⁺ and ‘used’ metal powders (powders that had already been used in a previous H₂ reaction) yielded more NADH in 1 h than pristine metal powder would in that time (Fig. S11). The same experimental order, but with the first step under Ar instead of H₂ lead to similar results. This could mean one of several things. On one hand, it is possible that the oxidised forms of the metals (Equations 1 and 2) are better catalysts for the hydrogenation reaction than the native metal forms. We performed additional experiments (16 h pretreatment with H₂, 4 h reaction time under H₂) with magnetite (Fe₃O₄), cobalt(II,III)oxide (Co₃O₄) and nickel(II)oxide (NiO) using the same amount of metal atoms per mol to test their ability to promote NAD⁺ reduction. In this case, however, no oxide yielded any NADH (Fig. S12). On the other hand, it is also possible that the 1 h reaction served as a pretreatment step (e.g. hydride formation on metal surfaces from either H₂ gas or oxidation of the metals), resulting in the observed higher yield of NADH after 1 h of reaction.

Discussion

We tested Fe, Co and Ni for their ability to reduce NAD⁺ with H₂ gas to establish a connection between

a biotic H[−] donor (NADH) and an abiotic donor (metal hydride). The reduction was performed by all three metals, which however showed differences in their reactivity and response to H₂-pretreatment. The detailed effects of H₂-pretreatment on each of the metals under the present conditions will be investigated further. In this publication, we were able to collect some insights concerning the possible mechanisms in the performed experiments.

Mechanisms: where do the hydrides come from?

Of all three metals, Ni produced the lowest (but still substantial) NADH yields with around 50% after H₂ pretreatment (Fig. 2C), but it employs the most straightforward hydrogenation mechanism, additionally backed up by the results of the experiments with heavy water. Known to enable the dissociation of H₂ [15,64–67], Ni was able to reduce NAD⁺ under H₂ gas and showed the strongest positive response to pretreatment with H₂ gas out of the three metals. This suggests that Ni-bound hydrides are transferred to NAD⁺ to produce mainly 1,4-NADH (s. Fig. 4A). The redox potentials calculated for the experimental conditions (40 °C, 5 bar H₂, pH 8.5) back up the observations (Equation S2) [68,69]: the potential of Ni(OH)₂ + 2 e[−] + 2 H⁺ ↔ Ni⁰ + 2 H₂O (E = −390 mV) is not reducing enough to enable 2 H₂O + 2 e[−] ↔ H₂ + 2 OH[−] (E = −510 mV).

Iron also dissociates H₂ to metal-bound hydrides, but can also produce fresh H₂ from water via metal-

bound hydrides under mild hydrothermal conditions [57,58,70]. This is consistent with the midpoint potential calculated for the experimental conditions: Fe(OH)₂ + 2 e[−] + 2 H⁺ ↔ Fe⁰ + 2 H₂O (E = −550 mV) [68], which is more negative than the redox potential for H₂ formation from H₂O (E = −510 mV). In our experiments, 100% NAD⁺ reduction was reached under all conditions after 4 h with Fe (Fig. 2A). The Fe reactions also benefit from pretreatment with H₂ gas, reaching high NADH yields in shorter times. The mechanistic effect of pretreatment, however, could not be determined. Through further experiments in heavy water (²H₂O) we were able to confirm that the reaction depends on the abundance of ¹H₂ gas: if the reactions take place under a 5 bar ¹H₂ atmosphere, surface dissociation of ¹H₂ seems to be the main pathway, while under Ar atmosphere freshly produced hydrides are apparently transferred from the metal surface (Fig. 4B). Fe is still visibly oxidised (formation of green rust Fe(OH)₂; Fig. S5) under the reducing H₂ atmosphere, but much less so than under Ar. We cannot exclude at this point that these oxidised forms of iron catalytically enhance the reaction with H₂ gas, but experiments we conducted with metal oxides as a proxy suggest they cannot promote NAD⁺ reduction by themselves (Fig. S12).

Following our preliminary report of metal-dependent NAD⁺ reduction with H₂ [71], it was recently reported [72] that iron sulfides can reduce small amounts of NAD⁺, but without an external

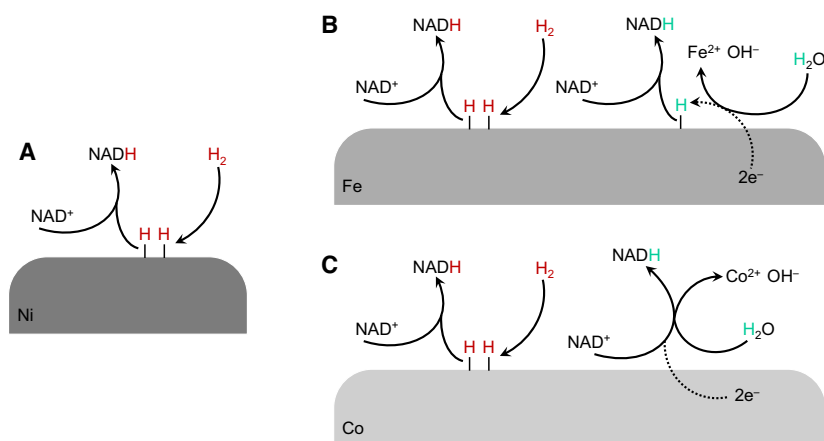


Fig. 4. Proposed mechanisms for NAD⁺ reduction depending on the used metal. (A) H₂ dissociates on the Ni surface. The metal-bound hydrides can then directly reduce NAD⁺ to NADH. (B) Fe employs two different mechanisms, depending on the availability of H₂ gas in the atmosphere. Without H₂, Fe itself delivers the electrons for hydride formation on its surface, the necessary proton comes from H₂O. With H₂ around, Fe is able to assist H₂ dissociation like Ni. (C) Co also is able to activate H₂ to transfer the hydride to NAD⁺. But without H₂ gas in the atmosphere, Co seems to employ a different mechanism than iron. Judging from the electrochemical potentials, it is able to reduce NAD⁺ directly without hydride formation. Note that the absorption of water molecules and/or hydroxides on the metal surfaces are not considered in these depictions.

electron source such as H₂, so the combination of both oxidised iron compounds such as iron sulfides, iron hydroxides or iron oxides and H₂ gas as electron donor has to be investigated further. In the conditions of serpentinizing hydrothermal vents, H₂ is abundant and ubiquitous [38,73], hence it is not clear what kinds of prebiotic environments such reactions in the absence [72] of H₂ would be modelling. In the presence of H₂ under the conditions reported here, NAD⁺ reduction is complete, rapid, and facile. Our experiments were performed under an excess of metal (1 M of metal to 3 mM NAD⁺, so 333 : 1), but lowering the amount of metal in relation to NAD⁺ (20 : 1 and 10 : 1, Fig. S3) did not automatically decrease the NADH yield by the same magnitude—at least for Fe and Co. This either means that the amount of metal does not directly influence the yield, underlining the catalytic character of the metals or that the NAD⁺ concentration is the limiting factor in our 333 : 1 experiments. Nickel is not spent during the reaction and depends on the abundance of H₂ to reduce NAD⁺ which strongly suggests that Ni is acting as a catalyst—an inorganic precursor of an enzyme, a geozyme—for the biochemical reaction. This made the drop of NADH yield between the 333 : 1 (50%) and 20 : 1 (1%) experiments surprising and suggests that the area of the hydrogenated Ni surface has to be quite large to efficiently reduce NAD⁺. As we also observed that Ni yields substantially more NADH under H₂ gas when the reactions take place in ²H₂O instead of H₂O (Fig. 3F), we posit that water molecules quickly cover Ni's surface and thus block the catalytic sites needed for H₂ dissociation. This also could explain why Ni is performing better when pretreated with H₂ before adding the aqueous NAD⁺/buffer: here, metal-bound hydrides can form before the binding sites are blocked by water molecules. Once NADH is being formed, these sites can be taken by water molecules again, which would explain why experiments with Ni do not exceed a 50% yield of NADH. Under geochemical conditions with lower water activity (also found in serpentinizing systems [74,75]), this process might be less of an issue than in the aqueous solutions investigated in our experiments.

Judging from our time-course experiments, we assumed that Co is also able to both dissociate H₂ and produce H₂ *in situ*, as pretreated Co gave the highest yield of 1,4-NADH in the shortest amount of time (Fig. 2B). Co is visibly far more dependent upon the presence of H₂ gas to attain higher NADH yields than Fe. But there is a third mechanism to be considered here, looking at the following midpoint potentials (calculated for the given experimental conditions)

[68,69,76]: although $\text{Co(OH)}_2 + 2 \text{e}^- + 2 \text{H}^+ \leftrightarrow \text{Co}^0 + 2 \text{H}_2\text{O}$ ($E = -407 \text{ mV}$) cannot directly enable $2 \text{H}_2\text{O} + 2 \text{e}^- \leftrightarrow \text{H}_2 + 2 \text{OH}^-$ ($E = -510 \text{ mV}$), it would be able to reduce $\text{NAD}^+ + 2 \text{e}^- + \text{H}^+ \leftrightarrow \text{NADH}$ ($E = -390 \text{ mV}$) directly. This might explain why we were not able to demonstrate both mechanisms for Co with the heavy water experiments as we could with Fe. Without H₂, Co did not show any reduction during the 2 h ²H₂O experiments. The data thus indicate that Co is able to dissociate H₂ [77] and transfer electrons to NAD⁺ (either in hydride form or directly), but the results concerning the possibility of a nascent H₂ pathway for Co are not conclusive (Figs. 3C,4C). In case Co is indeed directly transferring electrons to NAD⁺, there might be a kinetic inhibition in the ²H₂O experiments due to slower proton transfer [78].

In a geochemical context, it should be mentioned that in serpentinizing systems we can expect both abiotic hydride donor mechanisms to take place if the electron acceptor will permit: H₂ is constantly produced from H₂O on mineral surfaces (bound hydride intermediate) and dissolved H₂ gas (as a source for freshly chemisorbed hydride) is present in the hydrothermal effluent.

By separating the liquid and the solid phase mid-experiment we were trying to exclude homogeneous catalytic mechanisms (catalysis by metal ions in solution), which are known for hydrogenation reactions [9]. Our results indicate that reactions of the divalent metals do not play a major role in the present reactions. For Ni, this is in line with the role of Ni⁰ in the reaction mechanism of CODH proposed by Ragsdale (2009) [46], although in that reaction, electrons stem from ferredoxin rather than directly from H₂. We explicitly are not excluding colloidal hydroxides as potential catalysts for Fe and Co as we were not able to reliably separate them from the solid phase without changing the rest of the solid phase. However, experiments with Fe₃O₄, Co₃O₄ and NiO under H₂ atmosphere as a proxy for oxidised phases show that they do not promote NADH synthesis at all (Fig. S12).

NAD stability under alkaline conditions and the possibility for reversible reactions

In order to have been useful at life's emergence, NAD had to serve as both hydride donor and hydride acceptor. That means the oxidation/reduction reaction has to be able to proceed in both directions under the given environmental conditions. Very small pH fluctuations could bear upon this issue. From the present data (Fig. S7) we observe that NADH is more stable under (very) alkaline conditions than NAD⁺ which will degrade within a few hours under alkaline

conditions [54]. Also in our reduction experiments (at pH 8.5, usually increasing during the reaction), we observe a loss of NAD⁺ in reactions in which it is not quickly converted to substantial amounts of NADH (Table S1). Under slightly acidic conditions, however (pH < 7), NADH will be oxidised quite quickly. Thus, in an environment in which pH can slightly vacillate around neutral pH, both reduction and oxidation of NAD are possible. Mineral catalysts could probably direct the reversibility at even smaller pH ranges. In serpentinizing systems, local pH microenvironments have an influence on serpentinization rates [79], which might mean serpentinization rates could also have an influence on pH. Depending on the exact mineral composition of a serpentinizing system, pH depends on the buffering characteristics of mineral compounds, such that pH is not a static parameter. Under specific rock compositions, there are even a few acidic serpentinizing systems on modern Earth [38], although the chemical reactions of serpentinization are bound to ultimately make a hydrothermal system alkaline.

Abiotic and biotic hydride donors

Our study shows that metal surfaces can serve as abiotic hydrogenases (or ‘geozymes’) that can transfer the electrons from H₂ directly to an organic cofactor. This direct transfer of two electrons from H₂ to an organic cofactor, without intervention of one-electron transfer through FeS centres, has only been recently observed for a hydrogenase, namely the F₄₂₀ reducing [Fe] hydrogenase of methanogens and some anaerobic bacteria [22]. Metal hydrides could not only have served as abiotic hydride donors for biological molecules in early evolution, but also bring into focus a possible transition point from abiotic to biotic hydride donors in a prebiotic context. Prior to the origin of hydrogenases, early metabolic systems [6,26,80] were possibly still dependent upon metal hydrides from their geochemical surroundings but at some point an organic molecule that was able to integrate the hydride and transfer it to acceptors such as CO₂ under the given environmental conditions and made the protocell independent of metal hydrides. Though this is a strong hypothesis in need of testing, we note that there are cells living in H₂-rich environments today that appear to lack hydrogenases [39]. Our findings suggest that early redox cofactors might have interacted with H₂ rich environments in a far more complex manner than previously suspected. Our findings also show that in the case of Ni, an essential element of acetogens and methanogens [46], there exists a direct, rapid, and facile reaction between NAD⁺ and metal hydrides. Overall, H₂ gas is able to convert an organic molecule (NAD⁺) to an

organic hydride carrier (NADH) in the absence of enzymes [81], in the presence of native metals [41] under the conditions of H₂ rich hydrothermal vents, which naturally deposit native Ni (and Fe) in the form of the mineral awaruite (Ni₃Fe) [40,82,83].

Materials and methods

Samples with pretreatment

4 mmol of iron powder (Fe⁰; 99.9+ % metals basis, particle size < 10 µm, Alfa Aesar, Thermo Fisher Scientific, Lancashire, UK), cobalt powder (Co⁰; metal basis, particle size 1.6 µm, Alfa Aesar) and nickel powder (Ni⁰; metal basis, particle size 3–7 µm, Alfa Aesar) were placed in reaction glass vials, closed with a PTFE-membrane bearing crimp cap, equipped with a syringe needle for gas exchange, and lastly exposed to 5 bars of H₂ overnight (16 h, 400 r.p.m. and 50 °C) in a stainless-steel high-pressure reactor (BR-300, Berghof Products + Instruments GmbH, Eningen, Germany). Afterwards, for NAD⁺ reduction, a solution of 12 µmol of NAD⁺ (free acid, Merck Millipore, Darmstadt, Germany) in 4 mL of 1 M phosphate buffer (pH 8.5; potassium phosphate monobasic and sodium phosphate dibasic, Honeywell Fluka, Fisher Scientific, Schwerte, Germany; in HPLC-grade water) was prepared and added via a disposable syringe through the needle in the membrane, leading to an overall concentration of 1 M metal. As an experimental control, one additional sample was prepared for every reaction without any metal powder. The samples were reintroduced in the reactor, which was closed tightly and pressurised again with either 5 bar of Ar or 5 bar of H₂, depending on the experiment. For the controls with metal oxides (Fe₃O₄, 50–100 nm, 97% trace metals; Co₃O₄, < 10 µm; NiO, > 99.995% trace metals; Sigma-Aldrich, Taufkirchen, Germany) we used 1 M worth of metal atoms according to each oxide (0.333 M for Co₃O₄ and Fe₃O₄ and 1 M for NiO).

Samples without pretreatment

4 mmol of each metal powder were placed in 5 mL glass vials (beaded rim) with a polytetrafluoroethylene (PTFE)-coated stirring bar. The described NAD⁺ solution in phosphate buffer was pipetted on top, and sealed with a crimp cap with a PTFE-coated membrane. One more sample was prepared without metal powder to work as a control. To allow gas exchange between the interior and the exterior of the glass vial, a syringe needle was placed through the crimp cap membrane before the vials were placed in the high-pressure reactor.

Reaction

After pressurising the reactor with either 5 bar of Ar gas (99.998%, Air Liquide, Paris, France) or 5 bar of H₂ gas (99.999%, Air Liquide), the reactions were started and regulated by a temperature controller (BTC-3000, Berghof

Products + Instruments GmbH). Reactions were performed from 0.5 h to 4 h at 40 °C. After the reaction, the reactor was depressurised and the samples (metal powders and solution) were transferred to 2 mL Eppendorf tubes and centrifuged for 15 min at 16 000 *g*. (Biofuge fresco, Heraeus, Hanau, Germany). The supernatants (NAD⁺/NADH) and pellets (metal powders) were subjected to different analyses which are described below.

Separation of metal and supernatant to check for the active catalytic species

To study the liquid and solid phases separately, we separated them after a 1-h reaction with NAD⁺ (5 bar H₂, 40 °C) through hot filtration. The liquid phase was pipetted to a new glass vial with a new PTFE-coated stirring bar and sealed. The solid phase also went into a new glass vial but with a fresh NAD⁺ stock solution. Then, all-glass vials were re-introduced to the reactor to perform another 1-h reaction.

²H₂O controls

Three control experiments were made for Fe and Co: one for pretreatment under Ar, one for reactions with H₂, and another under Ar. Our controls contained ²H₂O instead of the corresponding volume of HPLC-grade water with all other parameters and analytic procedures maintained.

Measurement of pH

The pH after the reaction was measured for all samples containing inorganic catalysts using a Lab 875 Multiparameter Benchtop Meter (SI Analytics, Xylem, Mainz, Germany) and a pH electrode (SI Analytics).

Quantitative ¹H-NMR analysis

To detect and quantify the formation of NADH and side products such as nicotinamide and the decrease of NAD⁺ we used an existing protocol for quantitative proton nuclear magnetic resonance (¹H-NMR) [32,33]. The internal standard was a 7-mm solution of sodium 3-(trimethylsilyl)-1-propanesulfonate (97%, Sigma-Aldrich) in deuterium oxide (CH₃ peak at 0 p.p.m.; ²H₂O or D₂O, D₂O 99.9 atom % D, Sigma-Aldrich), mixed 1:6 with the supernatant of our samples. qNMR spectra were obtained on a Bruker (Billerica, MA, USA) Avance III 600 using a ZGESGP pulse program. Thirty-two scans were made for each sample with a relaxation delay of 40 s (600 MHz) and a spectral width of 12 315 p.p.m. (600 MHz). Analysis and integration were performed using MESTRENOVA (v.10.0.2) software.

UV-Vis Spectroscopy analysis

UV-Vis Spectroscopy was performed in some experiments as a complementary analysis to ¹H-NMR with an Agilent

Technologies (Santa Clara, CA, USA) Cary 300 UV-Vis Compact Peltier spectrometer. Two UV-Quartz cuvettes were used for each measurement, one containing the supernatant of a sample and the other 1 M phosphate buffer (pH 8.5) as a reference value. Analysis was made using the Cary UV Workstation.

Fourier Transform Infrared (FTIR) Measurements

The metals from a 4 h reaction under Ar in ¹H₂O were collected from their glass vials and individually washed with Milli-Q water through suction filtration. Then, the metal samples were dried using a vacuum desiccator overnight and homogenised with a mortar and pestle for analysis. FTIR spectra of the metal powders before and after the reaction were obtained on Perkin Elmer-Spectrum Two (Perkin Elmer, Waltham, USA) utilising an Attenuated Total Reflectance (ATR) geometry with a LaTiO₃ detector. For each measurement, the dry powder was directly measured on the surface of the ATR crystal at room temperature without any pretreatment. Each spectrum was collected with the resolution of 4 cm⁻¹ with 32 scans in the range of 400–4000 cm⁻¹.

Acknowledgements

MP thanks Kamila B. Muchowska, Joseph Moran, and Joana C. Xavier for discussions. MP, DPHP, JL and WFM thank the CeMSA@HHU (Center for Molecular and Structural Analytics @Heinrich Heine University) for recording the NMR-spectroscopic data. WFM and HT thank the Volkswagen Foundation (96_742) and the German Research Foundation (MA-1426/21-1 / TU-315/8-1). HT thanks the Max Planck Society for the basic funding. WFM thanks the European Research Council for funding (Advanced Grant EcolMetabOrigin 101018894).

Conflict of interest

The authors declare no conflict of interest.

Author contributions

MP and DPHP planned experiments; DPHP, TB, and JL performed experiments; MP and DPHP analysed data; MP and DPHP wrote the paper, WFM and KK edited the manuscript; WFM, KK, HT, AV provided supervision of the lab work.

Peer review

The peer review history for this article is available at <https://publons.com/publon/10.1111/febs.16329>.

Data availability statement

The authors confirm that the data supporting the findings of this study are available within the article and its supplementary materials. Original data files (¹H-NMR and FTIR spectra) are available on request from the corresponding author, MP.

References

- 1 Fuchs G. Alternative pathways of carbon dioxide fixation: Insights into the early evolution of life? *Annu Rev Microbiol.* 2011;**65**:631–58.
- 2 Sleep NH, Meibom A, Fridriksson T, Coleman RG, Bird DK. H₂-rich fluids from serpentinization: geochemical and biotic implications. *Proc Natl Acad Sci USA.* 2004;**101**:12818–23.
- 3 Porosoff MD, Yan B, Chen JG. Catalytic reduction of CO₂ by H₂ for synthesis of CO, methanol and hydrocarbons: Challenges and opportunities. *Energy Environ Sci.* 2016;**9**:62–73.
- 4 Thauer RK, Kaster AK, Seedorf H, Buckel W, Hedderich R. Methanogenic archaea: ecologically relevant differences in energy conservation. *Nat Rev Microbiol.* 2008;**6**:579–91.
- 5 Thauer RK, Kaster A, Goenrich M, Schick M, Hiromoto T, Shima S. Hydrogenases from methanogenic archaea, nickel, a novel cofactor, and H₂ storage. *Annu Rev Biochem.* 2010;**79**:507–36.
- 6 Weiss MC, Sousa FL, Mrnjavac N, Neukirchen S, Roettger M, Nelson-Sathi S, et al. The physiology and habitat of the last universal common ancestor. *Nat Microbiol.* 2016;**1**:1–8.
- 7 Sleep NH, Bird DK, Pope EC. Serpentinite and the dawn of life. *Philos Trans R Soc B Biol Sci.* 2011;**366**:2857–69.
- 8 Martin WF, Bryant DA, Beatty JT. A physiological perspective on the origin and evolution of photosynthesis. *FEMS Microbiol Rev.* 2018;**42**:205–31.
- 9 Kubas GJ. Fundamentals of H₂ binding and reactivity on transition metals underlying hydrogenase function and H₂ production and storage. *Chem Rev.* 2007;**107**:4152–205.
- 10 Kubas GJ. Molecular hydrogen complexes: coordination of a σ bond to transition metals bond. *Acc Chem Res.* 1988;**21**:120–8.
- 11 Ertl G. Primary steps in catalytic synthesis of ammonia. *J Vac Sci Technol.* 1983;**1**:1247–53.
- 12 Leigh GJ. Haber–Bosch and other industrial processes. In: Smith BE, Richards RL, Newton WE, editors. Catalysts for nitrogen fixation: nitrogenases, relevant chemical models, and commercial processes. Dordrecht: Springer; 2004. p. 33–54.
- 13 Kandemir T, Schuster ME, Senyshyn A, Behrens M, Schlögl R. The Haber-Bosch process revisited: on the real structure and stability of “ammonia iron” under working conditions. *Angew Chemie - Int Ed.* 2013;**52**:12723–6.
- 14 Pisarev AA. Hydrogen adsorption on the surface of metals. In: Gangloff RP, Somerday BP, editors. Gaseous Hydrogen Embrittlement of Materials in Energy Technologies Part 1. Woodhead Publishing Limited; 2012. p. 3–26.
- 15 Harris J, Andersson S. H₂ dissociation at metal surfaces. *Phys Rev Lett.* 1985;**55**:1583–6.
- 16 Harris J. Dissociation of H₂ on metal surfaces. *Langmuir.* 1991;**7**:2528–33.
- 17 Weiss MC, Sousa FL, Mrnjavac N, Neukirchen S, Roettger M, Nelson-Sathi S, et al. The physiology and habitat of the last universal common ancestor. *Nat Microbiol.* 2016;**1**:16116.
- 18 Thauer RK. Hydrogenases and the global H₂ cycle. *Eur J Inorg Chem.* 2011;**7**:919–21.
- 19 Fontecilla-Camps JC, Ragsdale SW. Nickel-iron-sulfur active sites: Hydrogenase and CO dehydrogenase. *Adv Inorg Chem.* 1999;**47**:283–333.
- 20 Lubitz W, Ogata H, Ru O, Reiherse E. Hydrogenases. *Chem Rev.* 2014;**114**:4081–148.
- 21 Siegbahn PEM, Tye JW, Hall MB. Computational studies of [NiFe] and [FeFe] hydrogenases. *Chem Rev.* 2007;**107**:4414–35.
- 22 Huang G, Wagner T, Ermler U, Shima S. Methanogenesis involves direct hydride transfer from H₂ to an organic substrate. *Nat Rev Chem.* 2020;**4**:213–21.
- 23 Buckel W, Thauer RK. Flavin-based electron bifurcation, ferredoxin, flavodoxin, and anaerobic respiration with protons (Ech) or NAD⁺(Rnf) as electron acceptors: A historical review. *Front Microbiol.* 2018;**9**:401.
- 24 Kurz LC, Frieden C. Anomalous equilibrium and kinetic α-Deuterium secondary isotope effects accompanying hydride transfer from reduced nicotinamide adenine dinucleotide. *J Am Chem Soc.* 1980;**102**:4198–203.
- 25 Klinman JP. The mechanism of enzyme-catalyzed reduced nicotinamide adenine dinucleotide-dependent reductions. Substituent and isotope effects in the yeast alcohol dehydrogenase reaction. *J Biol Chem.* 1972;**247**:7977–87.
- 26 Xavier JC, Hordijk W, Kauffman S, Steel M, Martin WF. Autocatalytic chemical networks at the origin of metabolism. *Proc R Soc B Biol Sci.* 2020;**287**:20192377.
- 27 Buckel W, Thauer RK. Energy conservation via electron bifurcating ferredoxin reduction and proton/Na⁺ translocating ferredoxin oxidation. *Biochim Biophys Acta - Bioenerg.* 2013;**1827**:94–113.
- 28 Fontecilla-Camps JC. Geochemical continuity and catalyst/cofactor replacement in the emergence and evolution of life. *Angew Chemie - Int Ed.* 2019;**58**:42–8.

- 29 Camprubi E, Jordan SF, Vasiliadou R, Lane N. Iron catalysis at the origin of life. *IUBMB Life*. 2017;**69**:373–81.
- 30 Preiner M, Xavier JC, Sousa FL, Zimorski V, Neubeck A, Lang SQ, et al. Serpentinization: Connecting geochemistry, ancient metabolism and industrial hydrogenation. *Life*. 2018;**8**:41.
- 31 McGlynn SE, Glass JB, Johnson-Finn K, Klein F, Sanden SA, Schrenk MO, et al. Hydrogenation reactions of carbon on Earth: Linking methane, margarine, and life. *Am Mineral*. 2020;**105**:599–608.
- 32 Preiner M, Igarashi K, Muchowska K, Yu M, Varma SJ, Kleinermaans K, et al. A hydrogen-dependent geochemical analogue of primordial carbon and energy metabolism. *Nat Ecol Evol*. 2020;**4**:534–42.
- 33 Varma SJ, Muchowska KB, Chatelain P, Moran J. Native iron reduces CO₂ to intermediates and endproducts of the acetyl-CoA pathway. *Nat Ecol Evol*. 2018;**2**:1019–24.
- 34 Saba T, Burnett JWH, Li J, Kechagiopoulos PN, Wang X. A facile analytical method for reliable selectivity examination in cofactor NADH regeneration. *Chem Commun*. 2020;**56**:1231–4.
- 35 Wang X, Yiu HHP. Heterogeneous catalysis mediated cofactor NADH regeneration for enzymatic reduction. *ACS Catal*. 2016;**6**:1880–6.
- 36 Kelley DS, Baross JA, Delaney JR. Volcanoes, fluids, and life at mid-ocean ridge spreading centers. *Annu Rev Earth Planet Sci*. 2002;**30**:385–491.
- 37 Schrenk MO, Brazelton WJ, Lang SQ. Serpentinization, carbon, and deep life. *Rev Mineral Geochem*. 2013;**75**:575–606.
- 38 Charlou JL, Donval JP, Fouquet Y, Jean-Baptiste P, Holm N. Geochemistry of high H₂ and CH₄ vent fluids issuing from ultramafic rocks at the Rainbow hydrothermal field (36°14'N, MAR). *Chem Geol*. 2002;**191**:345–59.
- 39 Suzuki S, Nealson KH, Ishii S. Genomic and in-situ transcriptomic characterization of the candidate phylum NPL-UPL2 from highly alkaline highly reducing serpentinized groundwater. *Front Microbiol*. 2018;**9**:1–13.
- 40 Klein F, Bach W. Fe-Ni-Co-O-S phase relations in peridotite-seawater interactions. *J Petrol*. 2009;**50**: 37–59.
- 41 Sousa FL, Preiner M, Martin WF. Native metals, electron bifurcation, and CO₂ reduction in early biochemical evolution. *Curr Opin Microbiol*. 2018;**43**:77–83.
- 42 Hawco NJ, McIlvin MM, Bundy RM, Tagliabue A. Minimal cobalt metabolism in the marine cyanobacterium *Prochlorococcus*. *Proc Natl Acad Sci USA*. 2020;**117**:15740.
- 43 Eckenhoff WT, Mcnamara WR, Du P, Eisenberg R. Cobalt complexes as artificial hydrogenases for the reductive side of water splitting. *Biochim Biophys Acta*. 2013;**1827**:958–73.
- 44 Ilic S, Pandey Kadel U, Basdogan Y, Keith JA, Glusac KD. Thermodynamic hydricities of biomimetic organic hydride donors. *J Am Chem Soc*. 2018;**140**:4569–79.
- 45 McCollom TM, Seewald JS. Serpentinities, hydrogen, and life. *Elements*. 2013;**9**:129–34.
- 46 Ragsdale SW. Nickel-based enzyme systems. *J Biol Chem*. 2009;**284**:18571–5.
- 47 Fuchs G. CO₂ fixation in acetogenic bacteria: variations on a theme. *FEMS Microbiol Lett*. 1986;**39**:181–213.
- 48 Xavier JC, Preiner M, Martin WF. Something special about CO-dependent CO₂ fixation. *FEBS Lett*. 2018;**285**:4181–95.
- 49 Degraaf RA, Behar KL. Detection of cerebral NAD⁺ by *in vivo* ¹H NMR spectroscopy. *NMR Biomed*. 2014;**27**:802–9.
- 50 Shabalin K, Nerinovski K, Yakimov A, Kulikova V, Svetlova M, Solovjeva L, et al. NAD metabolome analysis in human cells using ¹H NMR spectroscopy. *Int J Mol Sci*. 2018;**19**:3906.
- 51 Christmann K. Adsorption of hydrogen on a Nickel (100) surface. *Zeitschrift Für Naturforsch*. 1979;**34**:22–9.
- 52 Christmann K. Hydrogen transfer on metal surfaces. In: Hynes JT, Klinman JP, Limbach HH, Schowen RL, editors. Hydrogen-transfer reactions. Weinheim, Germany: Wiley-VCH Verlag GmbH & Co. KGaA; 2007. p. 751–86.
- 53 Christmann K. Interaction of hydrogen with solid surfaces. *Surf Sci Rep*. 1988;**9**:1–163.
- 54 Oppenheimer NJ. NAD hydrolysis: Chemical and enzymatic mechanisms. *Mol Cell Biochem*. 1994;**138**:245–51.
- 55 Rover LJ, Fernandes JCB, de Oliveira G, Kubota LT, Katekawa E, Serrano SHP. Study of NADH stability using ultraviolet–visible spectrophotometric analysis and factorial design. *Anal Biochem*. 1998;**55**:50–5.
- 56 Gayer KH, Woontner L. The solubility of ferrous hydroxide and ferric hydroxide in acidic and basic media at 25°. *J Phys Chem*. 1956;**60**:1569–71.
- 57 Fábos V, Yuen AKL, Masters AF, Maschmeyer T. Exploring the myth of nascent hydrogen and its implications for biomass conversions. *Chem - an Asian J*. 2012;**7**:2629–37.
- 58 Michiels K, Spooren J, Meynen V. Production of hydrogen gas from water by the oxidation of metallic iron under mild hydrothermal conditions, assisted by *in situ* formed carbonate ions. *Fuel*. 2015;**160**: 205–16.
- 59 Morawski B, Casy G, Illaszewicz C, Griengl H, Ribbons DW. Stereochemical course of two arene-cis-diol dehydrogenases specifically induced in *Pseudomonas putida*. *J Bacteriol*. 1997;**179**:4023–9.
- 60 Rowbotham JS, Reeve HA, Vincent KA. Hybrid chemo-, bio-, and electrocatalysis for atom-efficient deuteration of cofactors in heavy water. *ACS Catal*. 2021;**11**:2596–604.

- 61 Kasza RV, Griffiths K, Shapter JG, Norton PR, Harrington DA. Interaction of water with stepped Ni (760): Associative versus dissociative adsorption and autocatalytic decomposition. *Surf Sci.* 1996;**356**:195–208.
- 62 Zhou X, Wang L, Fan X, Wilfong B, Liou SC, Wang Y, et al. Isotope effect between H₂O and D₂O in hydrothermal synthesis. *Chem Mater.* 2020;**32**:769–75.
- 63 Farjamnia A, Jackson B. The dissociative chemisorption of water on Ni(111): Mode- and bond-selective chemistry on metal surfaces. *J Chem Phys.* 2015;**142**:234705.
- 64 Wang T, Ren D, Huo Z, Song Z, Jin F, Chen M, et al. A nanoporous nickel catalyst for selective hydrogenation of carbonates into formic acid in water. *Green Chem.* 2017;**19**:716–21.
- 65 Bhatia B, Sholl DS. Chemisorption and diffusion of hydrogen on surface and subsurface sites of flat and stepped nickel surfaces. *J Chem Phys.* 2005;**122**:204707.
- 66 Weng MH, Chen H, Wang Y, Ju S, Chang J. Kinetics and mechanisms for the adsorption, dissociation, and diffusion of hydrogen in Ni and Ni/YSZ Slabs: a DFT study. *Langmuir.* 2012;**28**:5596–605.
- 67 Christmann K. Hydrogen transfer on metal surfaces. In Hynes JT, Klinman JP, Limbach H-H, Schowen RL, editors. Hydrogen-transfer reactions. WILEY-VCH Verlag; 2007. p. 751–86.
- 68 Pourbaix M. Establishment and interpretation of potential-pH equilibrium diagrams of Fe Co, Ni. In Atlas of electrochemical equilibria in aqueous solutions. National Association of Corrosion Engineers; 1974. p. 307–343.
- 69 Haynes JW, Lide DR, Bruno TJ, editors. CRC Handbook of chemistry and physics, 93rd edn. Taylor and Francis Group: CRC Press; 2012.
- 70 Duo J, Jin F, Wang Y, Zhong H, Lyu L, Yao G, et al. NaHCO₃-enhanced hydrogen production from water with Fe and in-situ highly efficient and autocatalytic NaHCO₃ reduction into formic acid. *Chem Commun.* 2016;**52**:3316–9.
- 71 Pereira DPH, do Nascimento Vieira A, Kleinermmanns K, Martin WF, Preiner M. Serpentinizing systems and hydrogen activation in early metabolism. *Life.* 2021;**8**:41.
- 72 Weber JM, Henderson BL, LaRowe DE, Goldman AD, Perl SM, Billings K, et al. Testing abiotic reduction of NAD⁺ directly mediated by iron/sulfur minerals. *Astrobiology.* 2021;**22**:1–10.
- 73 Lang SQ, Brazelton WJ. Habitability of the marine serpentinite subsurface: a case study of the Lost City hydrothermal field. *Philos Trans R Soc A.* 2020;**378**:20180429.
- 74 Lamadrid HM, Rimstidt JD, Schwarzenbach EM, Klein F, Ulrich S, Dolocan A, et al. Effect of water activity on rates of serpentinization of olivine. *Nat Commun.* 2017;**8**:16107.
- 75 do Nascimento Vieira A, Kleinermmanns K, Martin WF, Preiner M. The ambivalent role of water at the origins of life. *FEBS Lett.* 2020;**594**:2727–33.
- 76 Huang H, Wang S, Moll J, Thauer RK. Electron bifurcation involved in the energy metabolism of the acetogenic bacterium *Moorella thermoacetica* growing on glucose or H₂ plus CO₂. *J Bacteriol.* 2012;**194**:3689–99.
- 77 Lewis EA, Le D, Murphy CJ, Jewell AD, Mattera MFG, Liriano ML, et al. Dissociative hydrogen adsorption on close-packed cobalt nanoparticle surfaces. *J Phys Chem C.* 2012;**116**:25868–73.
- 78 Huynh MHV, Meyer TJ, Cn CH, Nh DOM, Kno PF, The C. Colossal kinetic isotope effects in proton-coupled electron transfer. *Proc Natl Acad Sci.* 2004;**101**:13138–41.
- 79 McCollom TM, Klein F, Solheid P, Moskowitz B, Mccollom TM. The effect of pH on rates of reaction and hydrogen generation during serpentinization. *Philos Trans A.* 2020;**378**:20180428.
- 80 Weiss MC, Preiner M, Xavier JC, Zimorski V, Martin F. The last universal common ancestor between ancient Earth chemistry and the onset of genetics. *PloS Genet.* 2018;**14**:e1007518.
- 81 Muchowska KB, Varma SJ, Moran J. Nonenzymatic metabolic reactions and life's origins. *Chem Rev.* 2020;**120**:7708–44.
- 82 Plümper O, King HE, Geisler T, Liu Y, Pabst S, Savov IP, et al. Subduction zone forearc serpentinites as incubators for deep microbial life. *Proc Natl Acad Sci.* 2017;**114**:4324–29.
- 83 McCollom TM. Abiotic methane formation during experimental serpentinization of olivine. *Proc Natl Acad Sci USA.* 2016;**113**:13965–70.
- 84 Saba T, Li J, Burnett JWH, Howe RF, Kechagiopoulos PN, Wang X. NADH regeneration: a case study of Pt-catalyzed NAD⁺ reduction with H₂. *ACS Catal.* 2021;**11**:283–9.

Supporting information

Additional supporting information may be found online in the Supporting Information section at the end of the article.

Table S1. Single values of performed experiments.

Table S2. Relative quantity of ¹H atoms in the fourth position of the nicotinamide ring of NADH.

Fig. S1. Overview of experimental setup for timecourse NAD⁺ reduction experiments.

Fig. S2. Overview of ¹H-NMR spectra of all conducted experiments.

Fig. S3. Experiments with pretreated metals after 4 h at 40 °C under H₂ with a far lower concentration of metal powder.

Fig. S4. pH shift during experiments.

Fig. S5. Change of sample colouration during reaction.

Fig. S6. The effect of a higher concentrated buffer on pH stability and consequent NAD stability monitored via ¹H-NMR.

Fig. S7. Stability of NAD⁺ and NADH under different pH.

Fig. S8. FTIR measurements of Ni, Co and Fe before and after reaction.

Fig. S9. ¹H-NMR spectra of ²H₂O experiment with H₂-pretreated Fe under Ar.

Fig. S10. Schematic of hot filtration experiments.

Fig. S11. NADH synthesis before (Reaction 1) and after (Reaction 2) hot filtration.

Fig. S12. ¹H-NMR spectra of NAD⁺ with iron, cobalt and nickel oxides after reaction.

Equation S1. Calculation of H₂ concentration – Henry's law.

Equation S2. Calculation of electrochemical potential of H₂ at a given partial pressure and pH – Nernst equation.